Nov 8th, 12:00 AM

High Strength Steel Members with Unstiffened Compression Elements

Lan-Cheng Pan

Wei-wen Yu

Missouri University of Science and Technology, wwy4@mst.edu

Ninth International Specialty Conference on Cold-Formed Steel Structures
St. Louis, Missouri, U.S.A., November 8-9, 1988

HIGH STRENGTH STEEL MEMBERS WITH UNSTIFFENED COMPRESSION ELEMENTS

By L. C. Pan,[1] and W. W. Yu[2]

INTRODUCTION

In the past decade, high strength sheet steels have been widely used for automotive structural components and parts in order to obtain lighter and more fuel-efficient vechicles. A "Guide for Preliminary Design of Sheet Steel Automotive Structural Components" (1) was published by the American Iron and Steel Institute (AISI) in 1981. These design recommendations were primarily based on the 1968 AISI Specification (2) and were written for the design of cold-formed steel structural members with yield strengths up to 80 ksi. A new Automotive Steel Design Manual was published by the American Iron and Steel Institute in October 1986 (3). This Design Manual was prepared on the basis of the results of past and present research programs sponsored by the Institute. It can be used for materials with yield strengths up to 140 ksi.

In the first edition of the AISI Automotive Steel Design Manual, the effective width approach is employed for both stiffened and unstiffened compression elements with yield strengths up to 140 ksi. The effective width formulas included in this Design Manual are primarily based on the effective width equations used in the 1986 AISI Specification for the design of buildings (4). These formulas are based on the test results of sections with yield strengths not higher than 60 ksi (5). In order to apply the same effective width formulas with confidence to high strength materials, a further investigation is necessary.

This paper presents only the test results of sections with unstiffened elements fabricated from materials with yield strengths from 84.3 to 153.3 ksi. The test results of other researchers, using low strength materials, were also reexamined by using the effective width equations included in the 1986 AISI Specification. The modified effective width formula for predicting the ultimate strength of unstiffened elements is also presented.

EFFECTIVE WIDTH FORMULAS

Because the compression flanges of thin-walled structural members with relatively large w/t ratios can continue to carry increasing loads after the onset of local buckling of the compression elements and

---

[1]Structural Engineer, Thornton-Tomasetti, P.C., Engineers & Designers, New York, NY, Formerly Grad. Res. Assist., Dept. of Civ. Engrg. Univ. of Missouri-Rolla, Rolla, MO 65401.

[2]Curators' Prof. of Civ. Engrg., Univ. of Missouri-Rolla, Rolla, MO 65401.

because the complexity of the theoretical approaches was found to be too difficult to use in practical design, in 1932, von Karman (6) introduced a concept of "Effective Width" to determine the ultimate strength of thin metal sheets in aeronautical structures. In his approach, it was assumed that the entire load of the stiffened element is carried by two effective strips with a uniformly distributed stress equal to the edge stress, f_{max}, as shown in Fig. 1(a), instead of using the full width of the compression element with actual, nonuniform stress distribution.

In the 1940s, Winter performed extensive tests for the compression flanges of cold-formed steel sections at Cornell University. Based on his test results, Winter derived effective width formulas for the design of both stiffened and unstiffened compression elements under uniform compression. He also assumed that the entire load of the unstiffened element is to be carried by an effective strip with an uniformly distributed stress equal to the edge stress, f_{max}, as shown in Fig. 1(b), instead of using the full width of the compression element with a varying stress distribution. However, the effective width formula was not used for the design of unstiffened compression elements until the 1986 AISI Specification was published. The current effective width formula, based on Winter's equation (4,7), included in the 1986 AISI Specification for computing the load-carrying capacity of uniformly compressed elements is shown as follows:

$$b_e = w \quad \text{when} \quad \lambda \leq 0.673 \tag{1}$$

$$b_e = \rho w \quad \text{when} \quad \lambda > 0.673 \tag{2}$$

where b_e = effective width of a compression element
w = flat width of a compression element
$\rho = (1-0.22/\lambda)/\lambda$ (3)

λ is a slenderness factor determined as follows:

$$\lambda = (1.052/\sqrt{k})(w/t)(\sqrt{f/E}) \tag{4}$$

where f = the edge stress
E = modulus of elasticity, 29500 ksi (203,373 MPa)
k = plate buckling coefficient
= 4 for stiffened elements supported by a web on each longitudinal edge
= 0.43 for unstiffened elements supported by a web on one longitudinal edge and free on the other.

In the 1986 AISI Automotive Steel Design Manual, the above effective width formulas are also used to calculate the effective widths of fully stiffened compression elements without intermediate stiffeners and unstiffened compression elements.

EXPERIMENTAL INVESTIGATION

Eleven I-beams and 31 I-shaped stub columns were tested in this study. The ranges of w/t ratios used in this study were limited only from 5.6 to 53.3. All specimens were fabricated from three different types of high strength sheet steels (i.e., 80XF, 100XF, and 140SK). Table 1 gives the average values of mechanical properties including yield stress (F_y), proportional limit (F_{pr}), and tensile strength (F_u). It also lists the nominal thicknesses of all sheet steels used in the present experimental investigation. Note that the material 100XF is shown as 100XF(b) and 100XF(c) in Table 1. The letter "b" represents the material used to fabricate beam specimens. The letter "c" represents the material used to fabricate stub column specimens. As listed in Table 1, the material properties for 100XF(b) and 100XF(c) sheet steels are slightly different because these two materials were obtained from different heats.

A. TEST SPECIMENS

All steel sheets were sheared to the designed sizes before the channel sections were formed. All specimens were formed by a press brake operation with an inside bend radius of 1/4-in. at corners to prevent cracking.

1. I-Beams. Eleven I-beam specimens were tested using two different high strength materials (i.e., 80XF and 100XF(b)). I-shaped beam specimens were fabricated by connecting two identical channels back to back using self-tapping screws (#14 X 3/4-in.). The cross section of I-beam specimens is shown in Fig. 2. Table 2 gives the average cross-sectional dimensions of I-shaped beam specimens. The span lengths of beam specimens and the nominal thicknesses of sheet steels are also given in Table 2. The w/t ratios of unstiffened elements ranged from 6.5 to 22.5.

Sixteen foil strain gages were placed on the compression and tension flanges of I-shaped beam specimens for measuring compressive and tensile strains. The locations of strain gages (numbered from 1 to 16) placed on beam specimens are shown in Fig. 3. The location of section B-B as shown in Fig. 3 is at a distance about four times the width of the compression flange from midspan of the specimen.

2. Stub Columns. Thirty-one I-shaped stub-column specimens were also tested in this study using three different high strength materials (i.e., 80XF, 100XF(c), and 140SK). Figure 4 shows the cross section of an I-shaped stub column. Table 3 gives the average cross-sectional dimensions and lengths of stub-column specimens and the nominal thicknesses of sheet steels. The length of stub-column specimens is based on the criteria recommended in Ref. 8. The ranges of w/t ratios were (1) from 5.6 to 39.5 for 80XF, (2) from 6.8 to 49.1 for 100XF, and (3) from 9.6 to 53.3 for 140SK sheet steels.

The stub-column specimens were fabricated by bonding two identical channels back to back using a thin layer of PC-7 epoxy. Great care was

taken when the stub-column specimens were fabricated. If necessary, the ends of stub-column specimens were milled flat and parallel. As shown in Fig. 5, vertical bracings (3/4 X 3/4 X 1/8 in.) were attached to both sides of the web to assure that the web was fully effective. The vertical bracings were connected to the web by using 1/4-in. dia. bolts. The holes in the web were larger than the holes in the bracings so that no load could be transferred from web to bracings. Also, a thin layer of aluminum foil, coated with WD-40, was placed between each brace and web.

Fourteen foil strain gages were used to measure strains at the midheight of the stub-column specimens. The locations of strain gages are also shown in Fig. 5.

B. TEST PROCEDURE AND TEST RESULTS

All tests were performed in a 120,000 pound capacity Tinius Olsen universal testing machine. All specimens were loaded to failure.

1. I-beams. The test setup for I-beams is shown in Fig. 6. Lateral supports were applied to both sides of the compression flanges to prevent lateral buckling. Wood blocks were placed between flanges at loading points and at both ends to prevent premature failure of the web prior to beam failure.

The load was applied at quarter points of the beam specimen by a Tinius Olsen machine. Four-inch wide bearing plates were used under the loading points and at the ends of specimens. Load increments were about 10% of the predicted failure load of each specimen. At each load step, the load and corresponding strains were measured and recorded by the computer and the beam deflections were read from dial gages. The ultimate load of the specimen was read directly from the Tinius Olsen machine.

During the testing of I-beams, waving of the compression flange was observed as the load continued to increase beyond the buckling load. Curling of the compression flanges under loading plates was observed in most tests after buckling loads of specimens were reached. As expected, the specimen failed between the loading points. The beam specimen failed when the maximum strength of the compression flange was reached. Possible failure by flexural lateral buckling was prevented by providing lateral supports. Figure 7 shows typical flexural failure of I-beams with unstiffened elements.

2. Stub Columns. The test setup is shown in Fig. 8. At the beginning of the test, a small preload was applied to the specimen and the resulting strains were recorded for all strain gages to see whether the strain distribution was uniform over the cross section of the specimen. If necessary, thin layers of aluminum foil were added to the ends of the stub columns in the regions of low strain. This procedure was repeated until the strain distribution was essentially uniform over the cross section.

The load increments were about 10% of the predicted ultimate load. At

each load level, the load and corresponding strain readings were recorded and stored by the computer. Cross-head movement and lateral movements were also measured at each load level. The ultimate test load of the specimen was read directly from the Tinius Olsen machine when the specimen collapsed.

During the testing of stub columns, no bonding failure and no column buckling occurred prior to column failure. The failure mode of stub-column specimens with unstiffened elements varied with the width-to-thickness ratio of the unstiffened compression flanges. The unstiffened flanges with large w/t ratios showed large waving deformations, whereas the unstiffened compression flanges with small w/t ratios showed no noticeable waving until they failed. Typical failures of stub-column specimens with unstiffened compression flanges are shown in Fig. 9.

C. EVALUATION OF EXPERIMENTAL DATA

The results of tests obtained from this study were evaluated by comparing the tested failure loads to the predicted ultimate load-carrying capacities of structural members based on the current AISI effective width formulas. The test data of other investigators, using low strength materials, were reexamined by using the 1986 AISI Specification.

1. I-Beam Tests. For I-beams having equal flanges, the ultimate section strengths of such flexural members can be calculated on the basis of initiation of yielding of the compression flanges of the effective section. The ultimate section strengths of all I-beams can be calculated by using Eq. (5).

$$M_u = F_y S_e \tag{5}$$

where F_y = yield stress of steel
S_e = elastic section modulus of the effective section calculated with the extreme compression stress at F_y

The computed and tested ultimate moments of I-beams fabricated from 80XF and 100XF(b) steels are given in columns (2) and (4) of Table 4. The tested failure loads listed in column (1) were read directly from the testing machine when the specimens failed.

The results of beam tests performed by other investigators using low strength materials were compared with the predicted values calculated from the current AISI Specification (9). The average cross-sectional dimensions used to predict ultimate section strengths are also documented in Ref. 9.

Comparisons of the computed and tested ultimate moments are shown graphically in Fig. 10. Note that the current AISI Specification provides good agreements for all I-beams fabricated from 80XF and 100XF(b) sheet steels, while the computed ultimate moments of most of the specimens fabricated from low strength steels were smaller than the tested values (9).

2. Stub Column Tests. All the stub columns were subjected to uniform compression. Overall column buckling was prevented by the design of stub columns. The thickness of the web in a stub column was twice the thickness of the unstiffened compression flange because the stub columns were glued together at the webs. Vertical bracings were added to the web of stub columns if the webs were not fully effective stiffened elements based on the requirements of the current AISI Specification.

The ultimate load carrying capacities (P_u) of the stub-column specimens can be calculated from Eq. (6).

$$P_u = A_e F_y \tag{6}$$

where F_y = yield stress of steel
A_e = effective cross sectional area of the stub column for the maximum edge stress at F_y

The computed and tested failure loads of stub columns were compared in in column (4) of Table 5. Note that the failure loads of the specimens fabricated from 80XF sheet steels can be reasonably predicted by using the 1986 AISI Specification while the predicted failure loads of the specimens fabricated from 100XF(c) and 140SK steels are overestimated by the 1986 AISI Specification.

The results of tests performed by Dewolf (11) and Kalyanaraman (10) by using low strength materials are compared with the values predicted by using the current AISI Specification. The tested failure loads are about 23% greater than the failure loads predicted by using the current AISI Specification (9). The average cross-sectional dimensions used to predict ultimate failure loads are also documented in Ref. 9.

Figure 11 compares the computed and tested ultimate failure loads for sections fabricated from high and low strength materials. It can be seen that underestimation of the failure loads for sections fabricated from low strength materials became more pronounced as the w/t ratio of the unstiffened elements increased. Overestimations of the failure loads for sections fabricated from high strength materials, with yield stresses larger than 80 ksi, became more pronounced as the w/t ratio of the unstiffened elements increased. The effect of Fy on the prediction of the failure loads for stub columns with unstiffened flanges is shown in Fig. 12.

From a careful study of the test data obtained from the recent experimental investigation, it was found that the maximum edge stresses (f_{max}) of unstiffened elements were smaller than the yield stresses of steels when stub columns failed. The maximum edge stresses were determined from the maximum edge strains by using stress-strain curves. Strain gage readings were recorded at loads as close to failure as possible. Figures 13 and 14 compare the maximum edge stresses of unstiffened elements and the corresponding yield stresses. It can be

seen that the ratio f_{max}/F_y decreases as the w/t ratio of unstiffened elements and/or the F_y value increases.

MODIFICATION OF THE CURRENT AISI EFFECTIVE WIDTH FORMULAS

From the recent experimental investigation, it was found that the maximum edge stress (f_{max}) of an unstiffened compression flange in a structural member fabricated from high strength materials with yield stress higher than 84 ksi is smaller than the yield stress (F_y) of the steel at failure. As discussed earlier, the f_{max}/F_y ratio under the failure load is a function of the w/t ratio, the yield stress (F_y), and configuration of the cross section. The maximum edge stresses in the unstiffened elements are equal to a stress reduction factor, ϕ_u, times the yield stress of the steel (F_y). From the test results of the recent experimental investigation, stress reduction factors were developed as follows:

$$\phi_u = 1.079 - 0.6(\sqrt{w/t})(\sqrt{F_y/E}) \leq 1. \qquad (7)$$

where w = full width of an unstiffened element
t = thickness of sheet steel
F_y = yield stress of steel

Equation (7) is applicable only if the w/t ratio ranges from 5.6 to 53.3, the F_y value ranges from 84.3 to 153.3 ksi, and the value of $(\sqrt{w/t})(\sqrt{F_y/E})$ ranges from 0.128 to 0.526.

According to the effective design width concept, the yield stress is supposed to be the maximum edge stress for the unstiffened elements at failure. Therefore, modifications of the effective width formulas appear to be necessary for predicting the ultimate load carrying capacities of high strength steel members. By introducing a stress reduction factor into the effective width formulas, the effective widths, b_e, of an unstiffened element can be computed by using the following equations.

$$b_e = w \quad \text{when} \quad \lambda \leq 0.673 \qquad (8)$$

$$b_e = \rho w \quad \text{when} \quad \lambda > 0.673 \qquad (9)$$

where w = full width of a compression element

$$\rho = (1-0.22/\lambda)/\lambda \qquad (10)$$

λ is a slenderness factor determined as follows:

$$\lambda = (1.052/\sqrt{k})(w/t)(\sqrt{\phi_u F_y/E}) \qquad (11)$$

where E = modulus of elasticity, 29500 ksi (203,000 MPa)
k = buckling coefficient
= 0.43 for unstiffened elements
F_y = yield stress of steel
ϕ_u = stress reduction factor, determined from Eq. (7)

RECOMMENDED ANALYTICAL PROCEDURE

The analytical procedures, discussed earlier, for structural members fabricated from high strength sheet steels can also be modified by introducing the same reduction factor into the prediction equations. This modification reflects the experimental findings that the maximum edge stress of an unstiffened element at failure of high strength steel members was smaller than the yield stress of steel.

1. I-Beams. The ultimate moment capacity, M_u, of an I-beam can be computed by using the following modified equation.

$$M_u = \phi_u F_y S_e \tag{12}$$

where F_y = yield stress of steel
S_e = compression section modulus of the effective section calculated with extreme compression stress at $\phi_u F_y$, i.e. I_x divided by the distance from neutral axis to the extreme compression fiber.
ϕ_u = reduction factor determined from Eq. (7)

The computed ultimate section strengths of I-beams listed in column (3) of Table 4 were computed by using Eq. (12) with the reduction factor determined from Eq. (7). Comparisons of the tested and predicted ultimate section strengths are listed in column (6) of Table 4. It can be seen that the modified equations based on the present test results of stub columns also provide good agreements with the test values of beams. Note that only a limited range of w/t ratios was covered in this phase of investigation.

2. Stub Columns. The ultimate load carrying capacity of a stub column with unstiffened elements can be calculated by using the following equation.

$$P_u = \phi_u A_e F_y \tag{13}$$

where F_y = yield stress of steel
A_e = effective cross-sectional area of a stub column with maximum compression stress at $\phi_u F_y$
ϕ_u = reduction factor for unstiffened elements from Eq. (7)

The ultimate load carrying capacities of stub columns predicted by Eq. (13) are provided in column (2) of Table 5 for the stub columns fabricated from three different steels. Comparisons of the tested and predicted ultimate loads are given in column (5) of Table 5 and Fig. 15. From these comparisons, it can be seen that good agreements between tested and predicted ultimate load carrying capacity can be achieved for sections with yield stresses from 84.3 up to 153.3 ksi.

CONCLUSIONS

Based on the results of the recent tests, modified effective width formulas were proposed to predict the post-buckling strengths of unstiffened elements with yield stresses ranging from 84.3 to 153.3 ksi. Reasonable agreements were found between the predicted values and the test results of high strength steel members used in this study. However, the research findings discussed herein are limited only to the parameters covered in this study. Future investigations should be conducted to develop general design equations for different materials and cross-sectional configurations.

ACKNOWLEDGEMENTS

The financial assistances provided by the Department of Civil Engineering of the University of Missouri-Rolla, the American Iron and Steel Institute, and Dr. Yu's Curators Professorship are gratefully acknowledged. Materials used in the experimental study were donated by Bethlehem Steel Corporation, Inland Steel Company, and National Steel Corporation.

Computer facilities provided by Thornton-Tomasetti, P.C., Engineers and Designers for preparing this paper are also acknowledged. Special thanks are expressed to Ms. S. Handley, Ms. Y. Rivera, and Mr. E. Ling for helping on word processor and on printing this paper.

REFERENCES

1. American Iron and Steel Institute, "Guide for Preliminary Design of Sheet Steel Automotive Structural Components," 1981 Edition.
2. American Iron and Steel Institute, "Specification for the Design of Cold-Formed Steel Structural Members," 1968 Edition.
3. American Iron and Steel Institute, "Automotive Steel Design Manual," 1986 Edition.
4. American Iron and Steel Institute, "Specification for the Design of Cold-Formed Steel Structural Members," 1986 Edition.
5. Winter, G., "Strength of Thin Steel Compression Flanges," Bulletin No. 35, Part 3,Cornell University, Engineering Experiment Station, Ithaca, N.Y., 1947.
6. Von Karman, T., Sechler, E. E., and Donnell, L. H., "The Strength of Thin Plates in Compression," Transactions, ASME, Vol. 54, APM54-5, 1932.
7. Pekoz, T., "Development of a Unified Approach to the Design of Cold-Formed Steel Members," Report SG86-4, AISI, Washington, D.C., May 1986.
8. Johnston, B. G.,(ed.) Guide to Stability Design Criteria for Metal Structures, 3rd Edition, New York: John Wiley & Sons, Inc., 1976.

9. Pan, L. C., "Effective Design Width of High Strength Cold-Formed Steel Members," a Ph.D Dissertation, Civil Engineering Department, University of Missouri-Rolla, 1987.
10. Kalyanaraman, V., Pekoz, T., and Winter, G., "Unstiffened Compression Elements," Journal of Structural Division, ASCE, Vol. 103, No. ST9, September 1977.
11. Dewolf, J. T., "Local and Overall Buckling of Cold-Formed Compression Members," Structural Engineering Department, Report No. 354, Cornell University, Ithaca, NY, November 1973.
12. Cornell University, "Tests on Light Beams of Cold-Formed Steel," Second Summary Report, May 1943. (unpublished)
13. Yu, W. W., Santaputra, C., and Parks, M. B., "Design of Automotive Structural Components Using High Strength Sheet Steels," First Progress Report, Civil Engr. Study 83-1, Univ. of Missouri-Rolla, 1983.
14. Parks, M. B. and Yu, W. W., "Design of Automotive Structural Component Using High Strength Sheet Steels," Second Progress Report, Civil Engr. Study 83-3, Univ. of Missouri-Rolla, Aug. 1983. (Unpublished)
15. Santaputra, C. and Yu, W. W., "Design of Automotive Structural Component Using High Strength Sheet Steels," Status Report on Web Crippling Research, Civil Engr. Dept., Univ. of Missouri-Rolla, May 1985. (Unpublished)

NOTATION

The following symbols are used in this paper:

A_e = Effective cross-sectional area of stub columns
b_e = Effective width of a compression element
E = Modulus of elasticity of steel = 29,500 ksi
k = Buckling coefficient
M_u = Ultimate moment, in.-kips
P_u = Ultimate load, kips
S_e = Elastic section modulus of the effective section
t = Thickness of plate
w = Width of plat
F_y = Yield strength
f_{max} = Maximum edge stress of a compression element

Table 1 Material Properties and Thicknesses of Three High Strength Sheet Steels Used in the Experimental Study (13-15)

Material Designation	$(F_y)_c$ (ksi)	$(F_{pr})_c$ (ksi)	$(F_y)_t$ (ksi)	$(F_u)_t$ (ksi)	Elongation (%)	t (in.)
80XF	84.30	45.60	77.10	89.10	20.40	0.088
100XF(b)	113.10	72.00	113.10	113.10	8.10	0.062
100XF(c)	119.80	85.00	116.90	116.90	10.10	0.065
140SK	153.30	88.90	165.10	165.10	4.30	0.046

Notes:
1) $(F_y)_c$ and $(F_{pr})_c$ are based on longitudinal compression coupon tests.
2) $(F_y)_t$,$(F_u)_t$, and Elongation are determined from longitudinal tension coupon tests.
3) Elongation was measured over a 2-in. gage length.
4) 1 in. = 25.4 mm.
5) 1 ksi = 6.894 MPa.
6) XF represents low alloy, killed plus sulfide control steel. SK represents structural quality, killed steel.

Table 2 Dimensions of Beam Specimens with Unstiffened Flanges 80XF and 100XF(b) Sheet Steels

Specimen	BC (in.)	D (in.)	t (in.)	w/t	L (in.)	R (in.)
B80XFB2A	0.902	2.000	0.0870	6.503	39.00	0.25
B80XFB2B	0.904	1.990	0.0865	6.564	38.00	0.25
B80XFB4A	1.306	2.015	0.0875	11.074	38.00	0.25
B80XFB4B	1.305	2.020	0.0875	11.057	39.00	0.25
B80XFB6A	2.009	2.991	0.0875	19.103	39.00	0.25
B80XFB6B	2.008	2.988	0.0875	19.089	39.00	0.25
B100XFB18B	0.909	1.946	0.0645	9.222	36.00	0.25
B100XFB20A	1.254	2.515	0.0665	14.090	36.00	0.25
B100XFB20B	1.252	2.512	0.0655	14.298	36.00	0.25
B100XFB22A	1.825	2.932	0.0650	23.235	36.00	0.25
B100XFB22B	1.816	2.951	0.0655	22.546	36.00	0.25

Notes:
1) See Fig. 2 for definitions of symbols.
2) L is the span length of specimens.
3) 1 in. = 25.4 mm.

Table 3 Dimensions of Stub Columns with Unstiffened Flanges 80XF, 100XF(c), and 140SK Sheet Steels

Specimen	BC (in.)	D (in.)	t (in.)	w/t (in.)	Gross Area ($in.^2$)	L (in.)
80XFB7A	0.819	1.978	0.0845	5.740	0.5403	7.0
80XFB7B	0.818	1.985	0.0853	5.645	0.5460	7.0
80XFB9A	1.011	1.986	0.0858	7.844	0.6143	7.0
80XFB9B	1.012	1.987	0.0852	7.938	0.6114	7.0
80XFB11A	1.517	2.989	0.0868	13.614	0.9705	10.0
80XFB11B	1.516	2.985	0.0860	13.724	0.9620	10.0
80XFB13A	2.508	3.992	0.0885	24.514	1.5183	16.0
80XFB13B	2.507	4.002	0.0868	25.002	1.4912	16.0
80XFB15A	3.758	4.981	0.0868	39.461	2.0932	23.0
100XFB23A	0.765	1.997	0.0655	6.866	0.4131	7.0
100XFB23B	0.767	2.003	0.0663	6.806	0.4148	7.0
100XFB25A	1.110	1.994	0.0660	12.023	0.5065	7.0
100XFB25B	1.112	1.989	0.0660	12.064	0.5066	7.0
100XFB27A	1.509	3.018	0.0658	18.218	0.7416	10.0
100XFB27B	1.507	2.999	0.0650	18.335	0.7331	10.0
100XFB29A	2.513	4.004	0.0658	33.542	1.1338	16.0
100XFB29B	2.512	4.005	0.0652	33.693	1.1287	16.0
100XFB31A	3.522	4.998	0.0653	49.100	1.5237	22.0
100XFB31B	3.521	4.989	0.0654	49.015	1.5247	22.0
140SKB33A	0.746	2.002	0.0465	9.667	0.2944	7.0
140SKB33B	0.743	2.009	0.0463	9.637	0.2932	7.0
140SKB35A	0.988	2.042	0.0461	14.979	0.3411	7.0
140SKB35B	0.992	2.030	0.0465	14.952	0.3428	7.0
140SKB37A	1.499	2.999	0.0470	25.580	0.5328	10.0
140SKB37B	1.501	2.996	0.0472	25.612	0.5328	10.0
140SKB38A	2.001	4.002	0.0472	36.097	0.7244	13.0
140SKB38B	1.999	3.991	0.0467	36.452	0.7155	13.0
140SKB39A	2.507	3.984	0.0463	47.753	0.8029	16.0
140SKB39B	2.507	3.995	0.0467	47.428	0.8090	16.0
140SKB40A	2.763	3.986	0.0463	53.276	0.8504	17.0
140SKB40B	2.762	3.979	0.0463	53.260	0.8497	17.0

Note:
1) See Fig. 4 for definitions of symbols.
2) 1 $in.^2$ = 25.4 mm.
3) 1 $in.^2$ = 645.16 mm^2.

Table 4 Comparison of Computed and Tested Ultimate Moments Beam Specimens with Unstiffened Flanges Based on Eqs. (5) and (12), 80XF and 100XF(b) Sheet Steels

Specimen	P_u, kips	M_u, ft-kips			$\frac{(4)}{(2)}$	$\frac{(4)}{(3)}$
	test (1)	Based on Eq. (5) (2)	Based on Eq. (12) (3)	test (4)	(5)	(6)
B80XFB2A	6.25	27.867	27.789	30.469	1.093	1.096
B80XFB2B	6.50	27.576	27.489	30.875	1.120	1.123
B80XFB4A	7.60	35.238	34.431	36.100	1.024	1.048
B80XFB4B	7.48	35.200	34.396	36.441	1.035	1.059
B80XFB6A	12.20	68.024	64.619	59.475	0.874	0.920
B80XFB6B	14.05	68.452	65.053	68.494	1.001	1.053
Mean					1.025	1.049
Standard Deviation					0.079	0.063
B100XFB18B	5.50	25.868	25.113	24.750	0.957	0.986
B100XFB20A	9.35	42.758	40.571	42.075	0.984	1.037
B100XFB20B	8.70	41.870	39.691	39.150	0.935	0.986
B100XFB22A	12.85	56.443	51.685	57.825	1.024	1.118
B100XFB22B	12.70	58.620	53.815	57.150	0.975	1.062
Mean					0.975	1.037
Standard Deviation					0.030	0.049

Note:
1) 1 kip = 4.448 kN.
2) 1 ft - kip = 1.356 kN.m.

Table 5 Comparison of Computed and Tested Failure Loads Based on Eqs. (6) and (13) for Stub Columns with Unstiffened Flanges

Specimen	P_u, kips			(3)/(1)	(3)/(2)
	Based on Eq. (6) (1)	Based on Eq. (13) (2)	test (3)	(4)	(5)
80XFB7A	47.26	45.55	46.60	0.986	1.023
80XFB7B	47.79	46.03	46.40	0.971	1.008
80XFB9A	51.76	51.22	51.40	0.993	1.004
80XFB9B	51.43	50.90	51.10	0.993	1.004
80XFB11A	71.29	68.84	67.60	0.948	0.982
80XFB11B	70.51	68.06	67.90	0.963	0.998
80XFB13A	90.82	84.52	83.00	0.914	0.982
80XFB13B	88.78	82.48	85.60	0.964	1.038
80XFB15A	104.07	92.84	101.80	0.978	1.096
Mean				0.968	1.015
Standard Deviation				0.034	0.033
100XFB23A	49.178	45.10	48.21	0.917	0.935
100XFB23B	49.878	45.50	48.92	0.912	0.930
100XFB25A	52.364	47.60	49.88	0.909	0.954
100XFB25B	52.278	44.10	49.82	0.843	0.885
100XFB27A	69.121	65.70	63.93	0.951	1.028
100XFB27B	68.189	64.10	63.04	0.940	1.017
100XFB29A	85.688	79.90	74.68	0.932	1.070
100XFB29B	85.233	74.10	74.24	0.869	0.998
100XFB31A	Data is not reliable.				
100XFB31B	101.370	97.90	83.87	0.965	1.116
Mean				0.915	0.998
Standard Deviation				0.037	0.080
140SKB33A	41.522	34.90	39.41	0.841	0.886
140SKB33B	41.405	33.70	39.30	0.814	0.857
140SKB35A	Data is not reliable.				
140SKB35B	42.726	34.90	39.32	0.817	0.888
140SKB37A	57.874	55.60	50.45	0.961	1.012
140SKB37B	57.831	50.70	50.41	0.877	1.006
140SKB38A	72.929	52.80	60.64	0.724	0.871
140SKB38B	Data is not reliable.				
140SKB39A	71.232	52.80	56.64	0.741	0.932
140SKB39B	71.174	58.90	57.23	0.819	1.029
140SKB40A	71.300	57.80	55.58	0.811	1.040
140SKB40B	71.208	54.20	55.51	0.761	0.976
Mean				0.817	0.959
Standard Deviation				0.077	0.079

Note:
1) 1 kip = 4.448 kN.

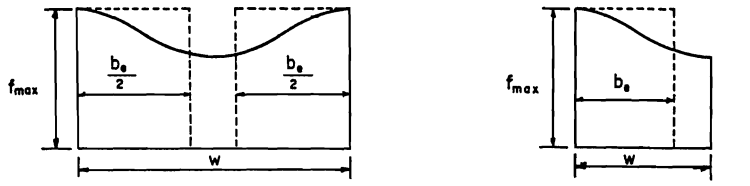

(a) Stiffened Element (b) Ustiffened Element

Fig. 1 Effective Design Width

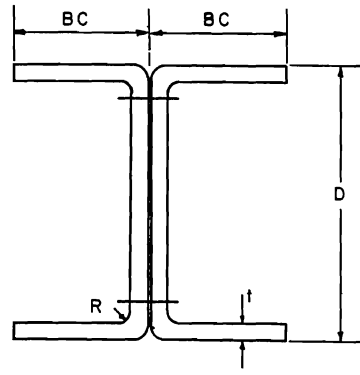

Fig. 2 Cross Section of I-Beam

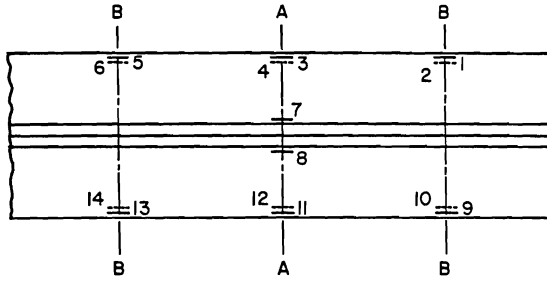

Top View

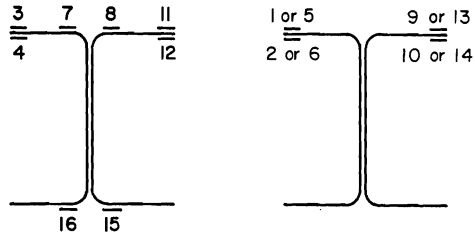

Section A-A
at Midspan

Section B-B

Fig. 3 Locations of Strain Gages on I-Beams

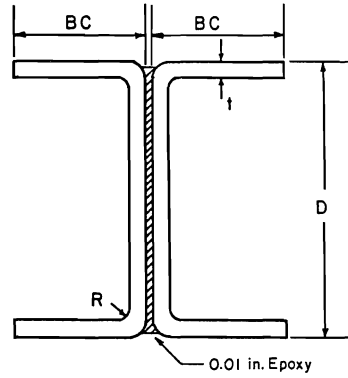

Fig. 4 Cross Section of I-Shaped Stub Columns

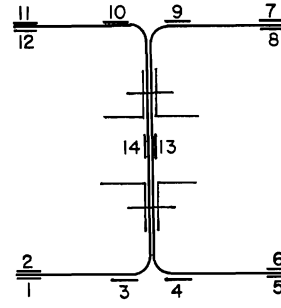

Fig. 5 Locations of Strain Gages on the I-Shaped Stub Columns

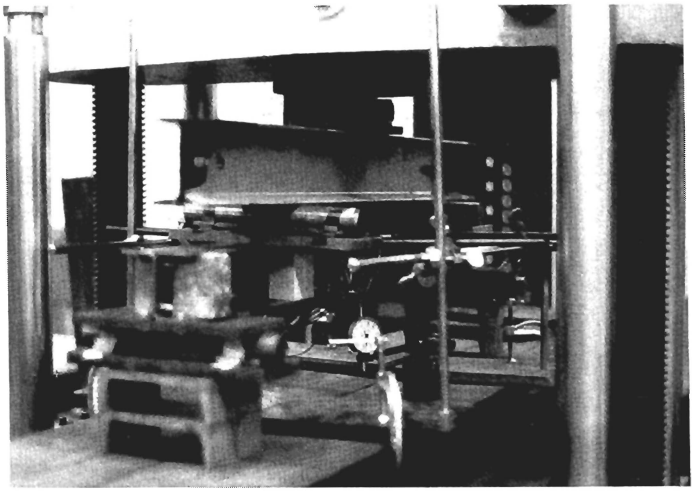

Fig. 6 Photo of Test Setup for I-Beams with Unstiffened Flanges

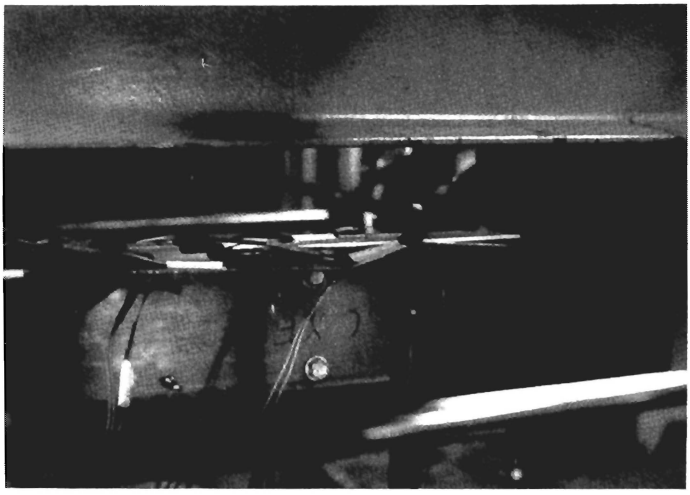

Fig. 7 Typical Failure of I-Beams with Unstiffened Flanges

Fig. 8 Test Setup of Stub Columns with Unstiffened Flanges

(a) Unstiffened Flange with Large w/t Ratio (Specimen 140SKB39A)

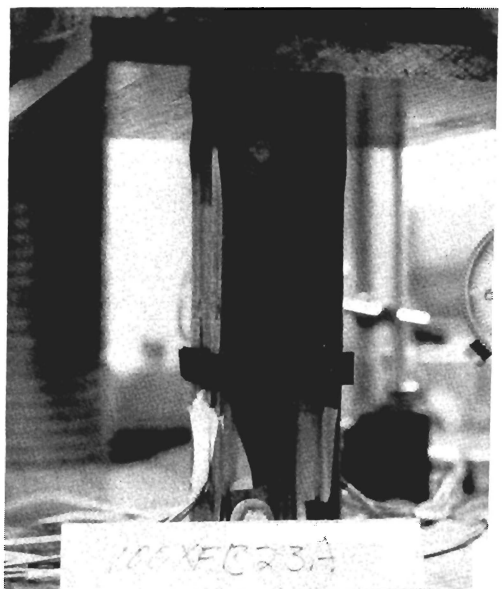

(b) Unstiffened Flange with Small w/t Ratio (Specimen 100XFB23A)

Fig. 9 Typical Failures of Stub Columns with Unstiffened Flanges

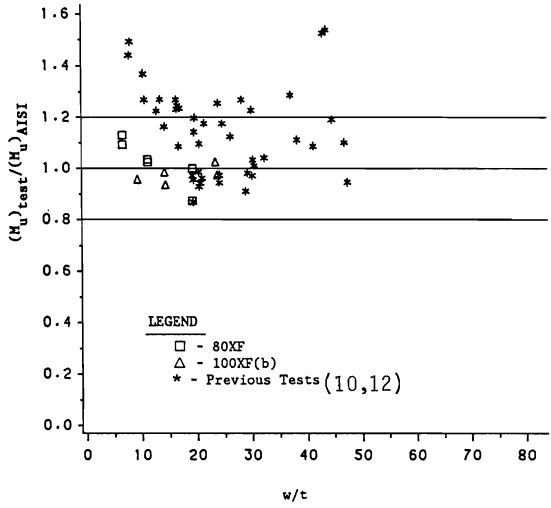

Fig. 10 Comparison of $(M_u)_{test}/(M_u)_{AISI}$ vs. w/t Beams with Unstiffened Flanges

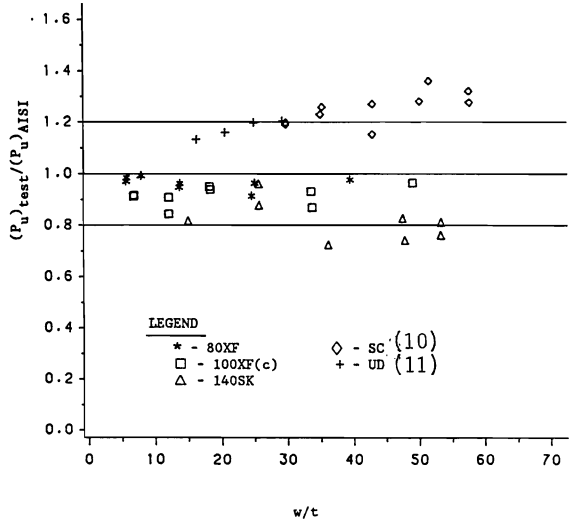

Fig. 11 Comparison of $(P_u)_{test}/(P_u)_{AISI}$ vs. w/t Stub Columns with Unstiffened Flanges

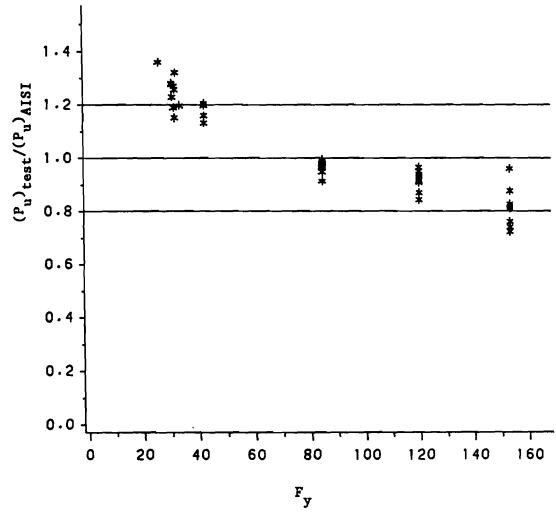

Fig. 12 Comparison of $(P_u)_{test}/(P_u)_{AISI}$ vs. F_y
Stub Columns with Unstiffened Flanges

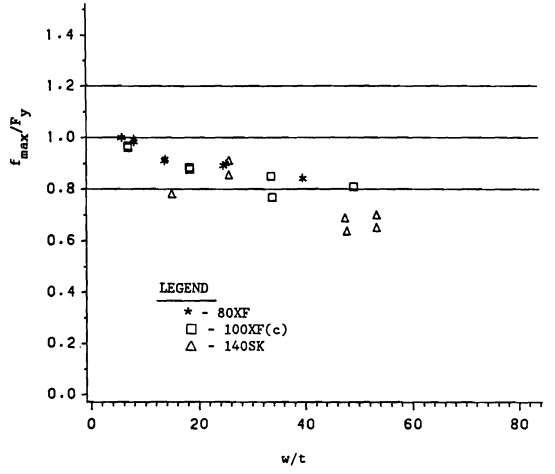

Fig. 13 Comparison of f_{max}/F_y vs. w/t
Stub Columns with Unstiffened Flanges

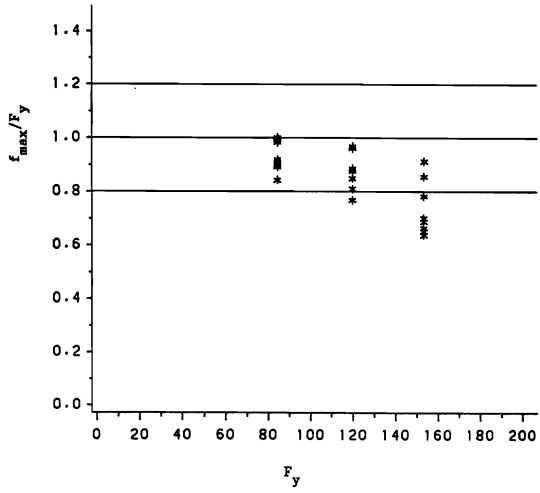

Fig. 14 Comparison of f_{max}/F_y vs. F_y
Stub Columns with Unstiffened Flanges

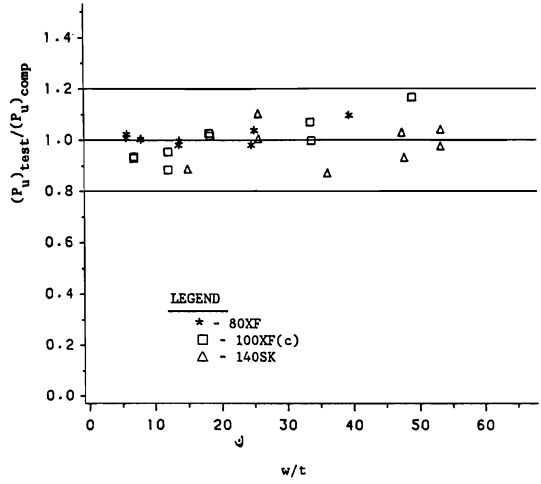

Fig. 15 Comparison of $(P_u)_{test}/(P_u)_{comp}$ vs. w/t
Stub Columns with Unstiffened Flanges
Based on Eq. (13)